# Structured multilayered electrodes of proton/electron conducting polymer for polymer electrolyte membrane fuel cells assembled by spray coating

André Wolz[a], Susanne Zils[a], Marc Michel[b], Christina Roth[a,*]

[a] Institute for Materials Science, TU Darmstadt, Petersenstr. 23, D-64287 Darmstadt, Germany
[b] Department of Advanced Materials and Structures, CRP Henri Tudor, 66 Rue de Luxembourg, L-4002 Esch-sur-Alzette, Luxembourg

## ARTICLE INFO

## ABSTRACT

Membrane electrode assemblies (MEAs) for fuel cell applications consist of electron conductive support materials, proton conductive ionomer, and precious metal nanoparticles to enhance the catalytic activity towards $H_2$ oxidation and $O_2$ reduction. An optimized connection of all three phases is required to obtain a high noble metal utilization, and accordingly a good performance. Using polyaniline (PANI) as an alternative support material, the generally used ionomer Nafion® could be replaced in the catalyst layer. PANI has the advantage to be electron and proton conductive at the same time, and can be used as a catalyst support as well. In this study, a new technique building up alternating layers of PANI supported catalyst and single-walled carbon nanotubes (SWCNT) supported catalyst is introduced. Multilayers of PANI and SWCNT catalysts are used on the cathode side, whereas the anode side is composed of commercial platinum/carbon black catalyst and Nafion®, applied by an airbrush. No additional Nafion® ionomer is used for proton conductivity of the cathode. The so called spray coating method results in high power densities up to $160\,\mathrm{mW\,cm^{-2}}$ with a Pt loading of $0.06\,\mathrm{mg\,cm^{-2}}$ at the cathode, yielding a Pt utilization of $2663\,\mathrm{mW\,mg_{Pt}^{-1}}$. As well as PANI, supports of SWCNTs have the advantage to have a fibrous structure and additional, they provide high electron conductivity. The combination of the new technique and the fibrous 1-dimensional support materials leads to a porous 3-dimensional electrode network which could enhance the gas transport through the electrode as well as the Pt utilization. The spray coating method could be upgraded to an in-line process and is not restricted to batch production.

© 2010 Elsevier B.V. All rights reserved.

## 1. Introduction

Polymer electrolyte fuel cells (PEMFCs) are expected to serve as a clean energy converter for portable, stationary and automotive applications in this century [1,2]. Their market introduction, however, is so far hindered due to the relatively high costs of the membrane, the catalysts, and the bipolar plates. The costly part of the catalysts is related to the amount of noble metal, which is mostly platinum. The use of carbon supported Pt and the use of Nafion® as a proton conductive media already helped to reduce the loading of Pt from 4 to $0.5\,\mathrm{mg\,cm^{-1}}$ in the electrode layer [3]. Another crucial point is the platinum utilization. In conventionally prepared membrane electrode assemblies (MEAs) only 10% of the available Pt is accessible [4]. Consequently, one of the most important aims in fuel cell research is to lower the Pt loading in accordance with a high Pt utilization.

The Pt utilization is related to the triple-phase boundary (TPB). The TPB is the unit of reactant, electrolyte and catalyst and is mainly responsible for the performance of a PEMFC [5]. The optimization of these interfaces is possible only by fine tuning the electrode structure at the nanoscale level. Therefore, several new techniques such as inkjet printing [6,7], sputtering [8], and others [9] have been developed to optimize the electrode assembly at a low platinum level.

For example, Taylor et al. [6] used the inkjet printing method to prepare electrode layers directly onto a Nafion® membrane. Here, the anode made of commercial Johnson Matthey 20% Pt/C catalyst with a loading of $0.021\,\mathrm{mg_{Pt}\,cm^{-2}}$ yielded a Pt utilization of $17,600\,\mathrm{mW\,mg^{-1}}$ in a $H_2/O_2$ fuel cell. In comparison, the performance of a sputtered fuel cell MEA strongly depends on the thickness of the catalyst layer [9]. O'Hayre et al. [10] obtained a peak in the performance of a MEA consisting of directly sputtered Pt films on both sides of a Nafion® membrane with a thickness of 5 nm. The corresponding loading of $0.014\,\mathrm{mg\,cm^{-2}}$ provides 60% of the power output of a commercial MEA. The need of ultra high vacuum conditions, special equipment and the limitation of Pt deposition

* Corresponding author at: Technical University of Darmstadt, Renewable Energies Group, Petersenstrasse 23, D-64287 Darmstadt, Germany.
Tel.: +49 6151 16 4391; fax: +49 6151 16 6023.
*E-mail addresses:* wolz@energy.tu-darmstadt.de (A. Wolz), su_zils@energy.tu-darmstadt.de (S. Zils), marc.michel@tudor.lu (M. Michel), c_roth@tu-darmstadt.de (C. Roth).

to only two dimensions are the drawbacks of the sputtering technique. The uniformity of sputtered films over a large area is another point which has to be taken into account.

In recent years another technique gained much attention for fuel cell applications: the layer-by-layer (LBL) assembly [11–13]. The LBL assembly was first published by Decher [14]. It follows the idea of alternately dipping glass substrates in oppositely charged polyelectrolyte solutions. This approach is time consuming due to the exposure time for the adsorption of the polyelectrolytes onto the substrate, this makes this approach not applicable for an in-line process. A faster way is to alternately spray the charged polyelectrolyte solutions onto a substrate [15]. This spraying technique speeded up the LBL assembly by a factor of over 100. Izquierdo et al. [16] compared the dipping with the spraying method and observed that spraying is suitable to produce films with reduced roughness. It also assembles homogeneous films in cases where dipping fails. The authors also suggested that the rinsing step could be skipped between each spraying step since drainage occurs during spraying. The sprayed LBL technique is suitable for the fabrication of PEMFC MEAs assembled of different catalyst materials. A previous study [12] with a sprayed LBL anode of Pt/PANI and Nafion® and sprayed commercial Pt/CB layer cathode supplied a power density of 63 mW cm$^{-2}$ at a Pt utilization of 437.5 mW mg$^{-1}$. Here, the amount of Pt used was almost two times lower than for standard carbon supported Pt catalyst MEAs.

The technique developed in this study is based on the sprayed LBL assembly. The main difference is the application of heat during the spraying process. This led to a speed up of the drying step when one layer is sprayed onto the membrane. Accordingly, no drain of the excess solvent occurs which could flush away the catalyst material. The idea behind this is the enhancement of the porosity in the layers and the prevention of material loss. Due to the simplicity of spraying alternating layers without rinsing, this method can be extended to an in-line fabrication process of MEAs.

One of the catalyst supports used in this study is polyaniline (PANI). It is one of the most studied conductive polymers in the last 100 years. Polyaniline is advantageous because of its good electron conductivity, high chemical stability in many environments and its simple protonating/deprotonating ability [17]. In some cases, the electron conductivity can exceed values above 100 S cm$^{-1}$ [18]. Its ability to be electron and proton conductive at the same time makes it possible to replace the Nafion® ionomer in the catalyst layer. Nevertheless, to date there is no existing publication about a successful replacement of Nafion® by proton conductive species, but the use of PANI as catalyst support has been reported in several publications [19,20] recently.

The standard carbon support corrodes in environments of high water content, acidic pH, elevated temperatures (50–90 °C), high potentials (0.6–1.2 V), and high oxygen concentration. The presence of platinum also accelerates the carbon corrosion [21]. All of these conditions are present at the cathode side of a PEMFC, so that, in the cathode layer carbon and water are transformed to carbon dioxide. As a result, support material is lost and the performance of the cell decreases and could lead to a total collapse of the electrode's porous 3D structure.

In contrary to carbon black, the use of carbon nanotubes can prevent carbon corrosion in a significant manner. Studies showed a high corrosion resistance of multi-walled carbon nanotubes connected with a lower loss of active Pt surface area at simulated cathode conditions in electrochemical experiments [22]. The fibrous structure and the high electron conductivity make it an ideal candidate as a fuel cell catalyst support and especially for the construction of 3-dimensional electrodes. In contrast to carbon supports, no degradation of the PANI support is expected during fuel cell operation. PANI showed its stability in several strong alkaline and acidic aqueous media [23]. Its good chemical stability is another advantage of the conductive polymer. Compared to other supports, PANI is a low-cost material which helps to further reduce fuel cell costs. The synthesis is performed via an interfacial polymerization reaction with aniline monomer and ammonium peroxydisulfate as oxidizing agent.

The introduction of a new MEA assembly technique with the potential of an in-line process scale up and the use of alternative catalyst support materials instead of carbon black are the main points of this work. Furthermore, this work aims a high Pt utilization at an adequate performance of the cell. The authors suggest that PANI does not suffer corrosion at the cathode. However, long-term test to verify this assumption has not been done yet and is not part of this work.

## 2. Experimental

### 2.1. Synthesis of polyaniline nanofibers (PANI-f) and their functionalization

All chemicals applied were of analytical grade and used as received without any further purification. Polyaniline fibers were prepared via an interfacial method described by Stejskal and Gilbert [24]. First, a solution of aniline (6 ml, J.T. Baker) and ammonium peroxydisulfate (3.6 g, SERVA) was dissolved in two beakers (200 ml) of 1 M hydrochloric acid, respectively. The ammonium peroxydisulfate solution was poured slowly into the aniline hydrochloride solution. The solution was kept at room temperature and was not stirred and not disturbed for at least 24 h. The PANI-fibers were filtrated with a Sartorius Polycarbonate (PC) track-etch membrane (mesh aperture 0.45 μm). The remaining PANI-f were washed with a sodium hydroxide (NaOH)-deionized water solution (pH of 12) to remove the Cl$^-$ counterions. Afterwards, the PANI-f were flushed with ethanol and 1 M sulfuric acid (H$_2$SO$_4$) solution for protonating the PANI to the emeraldine salt form and additionally washed with ethanol. The fibers were dried at 80 °C overnight.

The functionalization of PANI with platinum nanoparticles was achieved by the polyol method. As reducing agent ethylene glycol (EG, VWR) was chosen. The PANI-f (150 mg) were dissolved in EG (30 ml) with an ultrasonic disintegrator (Bioblock Scientific, 750 W). The pH of the dispersion was adjusted to 12 with 2 M NaOH–EG solution. Dihydrogen hexachloroplatinate(IV)hexahydrate (H$_2$PtCl$_6$, Sigma–Aldrich) with a concentration of 2 mg ml$^{-1}$ was dissolved in EG (20 ml) and added dropwise under mechanical stirring. The stirring was continued for 12 h and then the solution was heated up to 155 °C for 6 h under reflux. After cooling down, the pH of the solution was set to 2 with concentrated H$_2$SO$_4$, filtered with a polycarbonate filter (0.45 μm) and washed with ethanol. The wet powder was dried at 80 °C overnight.

### 2.2. Functionalization of single-walled carbon nanotubes

Elicarb® single-walled carbon nanotubes (150 mg, wetcake in water) from Thomas Swan & Co., Ltd., United Kingdom were used as catalyst support. The nanotubes were first treated in concentrated nitric acid (HNO$_3$) and H$_2$SO$_4$ (50:50) for 2 h to remove existing amorphous carbon and to create carboxyl, carbonyl and hydroxyl groups at the side walls of the tubes. After purification the concentrated acids were carefully diluted with deionized (DI) water and filtered via a PC-membrane (0.2 μm). During filtration the nanotubes were additionally rinsed with DI water and ethanol, until the pH of the rinsing solution was nearly neutral.

The nanotubes were not dried prior the functionalization with metal nanoparticles and afterwards dispersed in EG (30 ml) with the help of an ultrasonic disintegrator. The dispersion was mechani-

cally stirred and hexachloroplatinate acid ($2 \, mg \, ml^{-1}$) in EG (20 ml) was added slowly via a dropping funnel. The stirring was continued for 12 h. The dispersion was heated to 155 °C for 3 h under reflux. After cooling down to room temperature the solution was filtered via a PC-membrane (0.2 μm), washed with ethanol and MilliQ water. The Pt/SWNCT catalyst was stored in wet condition to prevent an agglomeration of the nanotubes.

## 2.3. Materials characterization

The conductivity of PANI was measured with the van der Pauw [25] method on thin films sprayed on glass substrates of $1 \times 1 \, cm^2$ and connected to a power source with gold contacts. The PANI-f were dispersed in isopropanol with a pH of 2.6 to obtain optimal dispersion [26] and to keep the PANI-f in their conductive emeraldine form. The thickness of the film was recorded with a Dektak IIA surface profile measuring system.

Thermogravimetric analysis was used to determine the precious metal loading on the different supports materials. The measurements were performed with a Netzsch STA 449C Jupiter under synthetic air (Linde®, $80\% \, N_2$–$20\% \, O_2$) atmosphere in a range from 30 to 1035 °C with a heating rate of 5 °C min$^{-1}$.

The different catalyst materials were characterized by X-ray powder diffraction (XRD). The diffractometer used was a STOE STADI-P with Germanium monochromized Cu Kα-radiation ($\lambda = 1.54060 \, Å$) and a position-sensitive detector with an aperture of 40°. The average particle sizes of the nanoparticles were obtained with a Rietveld fit of the measured pattern and the Cagliotti equation or with a Gauss fit on the (2 2 0) Bragg reflection.

In addition to the XRD measurements, the particle size and the dispersion of the particles on the support were observed with transmission electron microscopy performed at a FEI CM200 equipped with a LaB$_6$ filament and an acceleration voltage of 200 kV. For the multilayer morphology investigations thin cross-sections of the MEA were prepared using ultramicrotomy [27] and studied with transmission electron microscopy.

Scanning electron microscopy (SEM) investigations were carried out with a FEI Quanta 200 FEG, equipped with a field emission gun and operating at 15 kV.

## 2.4. Multilayer MEA preparation

As polymer exchange membranes a Nafion® 117 (thickness 183 μm) sheet was purchased from Ion Power Inc., New Castle, DE, USA. The membranes ($9 \times 7 \, cm^2$) were treated according to a standard preparation procedure before spraying. In order to remove organic impurities and to switch the membrane to the required H$^+$ form, the membranes were boiled in 50 vol.% HNO$_3$ and DI water for 1 h, rinsed in boiling DI water for 30 min, boiled in 0.5 M H$_2$SO$_4$ solution for 30 min and boiled twice in MilliQ water for 30 min, respectively. The membranes were stored in MilliQ water after activation.

One side of the MEA consists of a multilayered electrode. For the multilayer assembly two separate inks were prepared. The first ink contained PANI (100 mg) supported catalyst dispersed in ethanol (50 ml). Sonication was applied until a good dispersion was achieved. The best dispersion was obtained using a solvent at a pH of 2.6 as described by Li and Kaner [26]. The second ink consisted of carbon nanotubes (100 mg) dispersed in DI water (12.5 ml, pH adjusted to 12 with NaOH solution), and ethanol (37.5 ml) was added accordingly.

The multilayer assembly was done at 120 °C using ecoSpray® spraying containers (Labo Chimie, France) for an electrode area of $5 \times 5 \, cm^2$. The Nafion® membrane was fixed in a spraying mask standing upright, perpendicular to the spraying cone. The spray

coating technique was carried out as follows. As the first layer, PANI supported catalyst was sprayed for 4 s onto the Nafion® membrane. After spraying, additional 2 s was waited, allowing the layer to dry completely. As the following layer, carbon nanotubes supported catalyst was sprayed for 4 s. This alternating procedure was repeated, until the spraying containers were completely empty. The layers were sprayed in zig-zagging motion by hand, until the whole membrane area was homogeneously covered. The unity of one PANI and one SWCNT layer is named bilayer. With the used amount of ink it was possible to spray around 40 bilayers.

For the opposite electrode of the MEA commercial 20% Platinum on carbon black (CB) (Johnson Matthey Plc) was used. The ink contained Pt/CB (200 mg), Nafion® 117 solution (1 ml, Sigma–Aldrich), MilliQ water (9 ml), isopropanol (40 ml), and 2 drops of glycerine. The ink was homogenized by the ultrasonic disintegrator and sprayed onto the membrane at 120 °C using a spraying container.

## 2.5. Single-cell tests

The polarization curves of the MEA were collected in a home built manually operated fuel cell test bench. The MEA was placed between two gas diffusion layers (Toray® Carbon Paper TGP-H-090, 60 wt.% wet proofing) without any external pressure applied, sealed with Teflon® gaskets and surrounded by graphite plates with a column gas flow pattern. The current collectors consist of gold coated stainless steel plates.

The multilayered side was used as the cathode and the Pt/CB side as the anode, respectively. At the anode hydrogen (Linde®, N5.0) with a flow rate of 183 ml min$^{-1}$ was mixed with water in a humidifier ($T = 80$ °C). The cathode was fed with high-purity oxygen (Linde®, N4.5) at 86 ml min$^{-1}$. The cell temperature was set to 75 °C and the humidifier temperature to 80 °C. The MEA was conditioned before collecting a polarization curve.

## 3. Results and discussion

PANI-f were synthesized via a interfacial polymerisation reaction by just mixing an aqueous solution of aniline and an oxidant. The method and its reproducibility are described in the literature [26,28]. Li and Kaner [28] discovered that agitation or shaking inhibits the fibre formation and results in granular PANI particles. In this study, the reaction was done without any agitation or shaking to provide ideal conditions for the fibre formation. To obtain fibers instead of granular particles is important with respect to a controllable buildup of a 3D electrode's structure. The reaction conditions in our studies with an aniline to ammonium peroxydisulfate molar ratio of 4:1 led to fibrous PANI. TEM observations support these findings and shows PANI-f with an average diameter of approx. 50 nm and a length of several microns. The strong bundling of the fibers makes it impossible to measure the exact length.

Electric conductivity was obtained by the van der Pauw method on a thin PANI-f film, sprayed on a glass substrate. The average film thickness was measured to be 6.9 μm. With this value a specific film conductivity of 0.07 S cm$^{-1}$ was calculated. The electrical conductivity of the sprayed film is considerably lower than in situ grown PANI films on glass, which can exceed conductivities of 18.8 S cm$^{-1}$ at a thickness of 109 nm, if prepared in 1 M HCl [29]. The high specific electrical resistance of the sprayed film could be explained by insulating barriers between the conductive islands of PANI due to inhomogeneities.

In order to use PANI-f as catalyst in a PEMFC MEA, the fibers have to be functionalized with platinum nanoparticles. An optimum catalytic activity of the Pt particles is reached when the Pt particle sizes range between 3 and 5 nm [30]. The particles also should have a homogeneous distribution on the support. The decoration of the
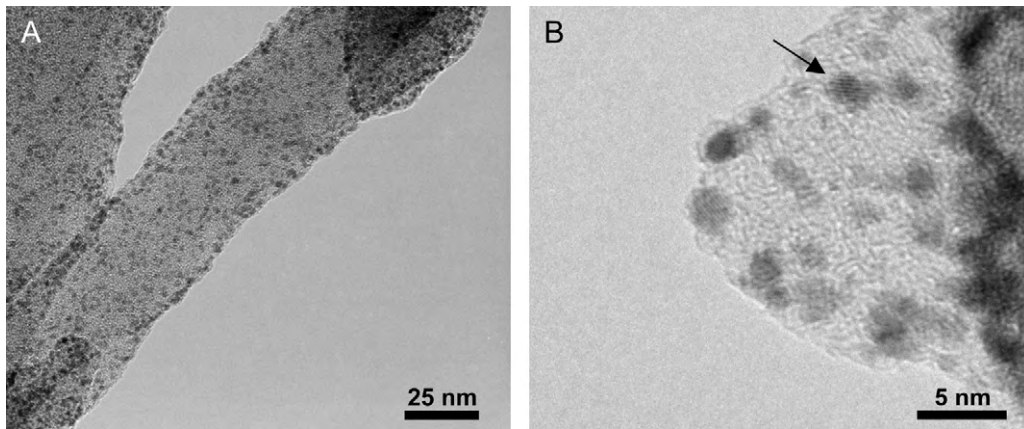
**Fig. 1.** TEM micrographs of PANI decorated with Pt nanoparticles with a Pt loading of 9.7 wt.% (A) overview and (B) in detail.

PANI support is carried out in situ by the ethylene glycol method, in which, the $Pt^{4+}$ ions of the precursor ($H_2PtCl_6$) are reduced by ethylene glycol to $Pt^0$ [19]. The TEM micrograph in Fig. 1(A) gives an overview of the homogeneous distribution of the Pt nanoparticles on the entire length of the PANI-f. A high magnification TEM picture in Fig. 1(B) shows several lattice planes of a Pt (marked with an arrow) even in the nanometer range of the particles.

The crystalline Pt particles allow a particle size determination via X-ray diffraction (XRD). The corresponding pattern is shown in Fig. 2. The characteristic (1 1 1), (2 0 0), (2 2 0), and (3 1 1) Bragg reflections for face-centered cubic (fcc) platinum can easily be seen in the pattern. As the reflections are broadened, a Rietveld refinement was not applicable. Therefore, the full-width at half maximum ($B_{2\theta}$) of the (2 2 0) reflection was estimated via a Gaussian fitting curve (see insert in Fig. 2). The average particle size $d$ was calculated by the Scherrer equation.

$$d = \frac{k\lambda}{B_{2\theta}\cos\theta}$$

Here $k$ is a shape coefficient (0.9), $\lambda$ is the X-ray wavelength (Cu $K_\alpha$, $\lambda = 1.54060$ Å), and $\theta$ is the angle at the position of the peak maximum (°). The mean Pt particle size for Pt/PANI is 4.0 nm, which was also confirmed by TEM. Within several experiments in our group the shift in particle sizes for polyol depositions at the same support were of the same size.
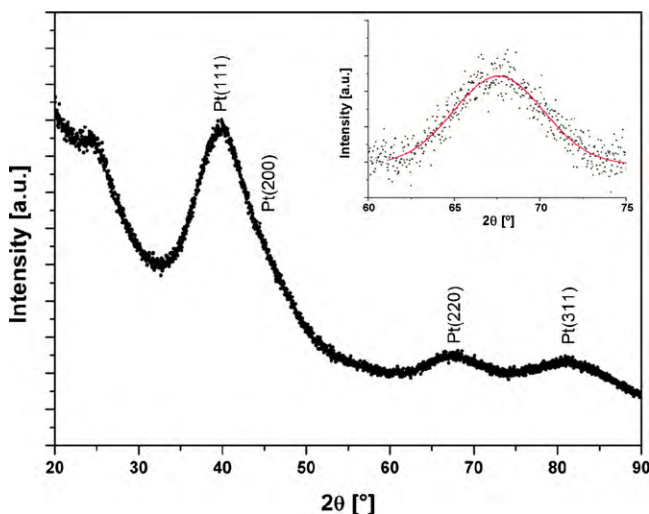
Thermogravimetric analysis of Pt/PANI revealed a loading of 9.7 wt.%. The loading was obtained by calculating the actual Pt mass of the remaining PtO after heating the Pt/PANI up to 1000 °C. The ratio of the remaining total mass of Pt and the weight of the support is specified as loading of the catalyst.

The decoration of SWCNT with Pt was carried out via the polyol method as well. The reaction conditions are slightly different to PANI catalysts because from our experience, the Pt is dispersed more easily on SWCNT than on PANI-f. Therefore, a particle size of 3–5 nm is obtained within the half of the heating time at the same temperature. The collected XRD pattern of Pt/SWCNT is shown in Fig. 3. A Rietveld refinement of the obtained pattern resulted in a mean Pt particle size of 4.8 nm. The loading was calculated to be 14.5 wt.% by TGA.

In order to arrange a multilayer setup with a high homogeneity an important point is to use well dispersed inks. To prevent agglomeration during ink preparation and spraying, all supports were used in wet condition during the production process. The particular pH adjustment of the solvents for PANI-f and SWCNTs resulted in a high level of catalysts' unbundling.

The multilayer electrode was directly assembled onto a Nafion® 117 membrane. Following the LBL procedure of Michel et al. [12], alternating layers of the positively charged Pt/PANI and the negatively charged Pt/SWCNT polyelectrolytes were sprayed. The application of temperatures of 120 °C during spraying is the main
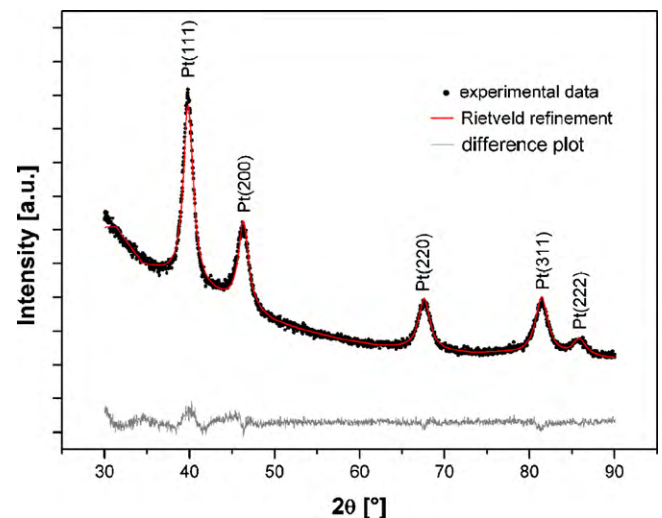


**Fig. 2.** XRD pattern of Pt/PANI measured with Cu $K_\alpha$ radiation ($\lambda = 1.54060$ Å) and magnified Pt(2 2 0) Bragg reflection with Gaussian fitting curve (inset).



**Fig. 3.** XRD pattern with Rietveld refinement of Pt/SWCNT measured with Cu $K_\alpha$ radiation ($\lambda = 1.54060$ Å).
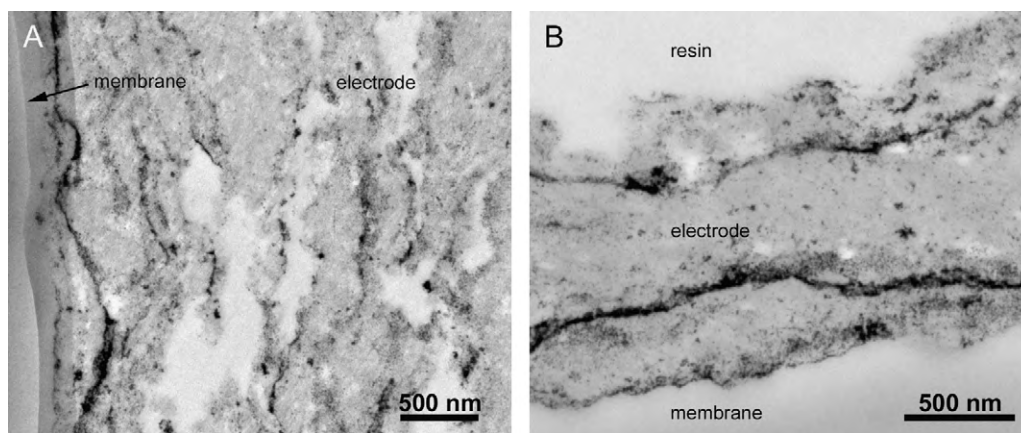
**Fig. 4.** TEM micrographs of cross-sections of Pt/SWCNT–Pt/PANI.

difference to the conventional LBL technique, where spraying is done at temperatures up to 40 °C. The elevated temperature results in a higher evaporation rate and avoids a drainage of excess material. Instead of a catalyst loss of 99% occurring at conventional LBL [15], with our technique it was possible to deposit 6.3% of the starting material onto the membrane. It has already been shown [13], that the high losses at conventional LBL occur due to the fact that just monolayers of the polyelectrolyte adsorb at the surface. In this work, the heating applied during the spray coating prevents the drainage of excess material after spraying, and so, more than a monolayer sticks on the surface. Altogether, the membrane consists of 39 bilayers, where one bilayer is equivalent to one Pt/PANI and one Pt/SWCNT layer. Hence, the weight of one single layer is 0.16 mg.

TEM micrographs of the multilayer electrode are shown in Fig. 4. The overview pictures (Fig. 4(A) and (B)) indicate that the intended layered structure of the electrode was obtained. The large distance between the separate layers is different and believed to arise from the preparation technique, where resin is used to embed the MEA. The resin probably pulls the layers apart. Therefore, the embedded MEAs are not favored for electrode thickness measurements. TEM observations show that the individual layers cannot be indentified easily.

The SEM micrograph of a Pt/SWCNT–Pt/PANI multilayer electrode cross section (Fig. 5) reveals an electrode thickness of 6.6 μm. The MEA was prepared in liquid nitrogen for SEM observations.
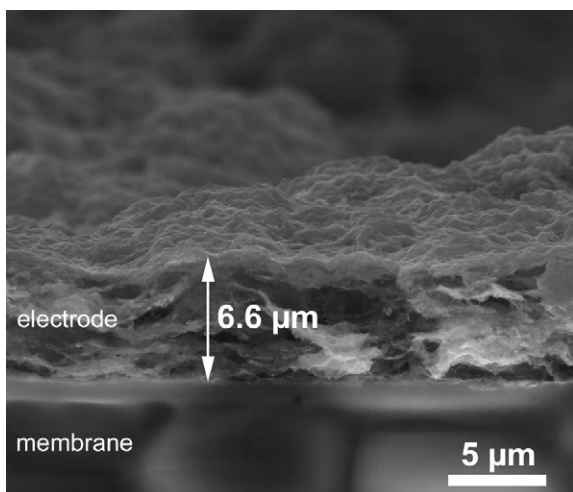
Regarding the 39 bilayers, each sprayed bilayer increased the thickness by 169 nm. The picture also indicates a quite rough surface of the electrode, which could be an indication of a high electrode porosity. The 3D network derives from the strong interpenetration of the single layers, where newly sprayed layers interpenetrate the already assembled network. This creates a strong contact of electron and proton conductive species in the layers. By changing the spraying duration, which is consistent with the amount of impacting material at the membrane surface, the penetration, and accordingly the proton conductivity can be tuned.

Sapurina and Stejskal [31] showed that the electron conductivity of PANI/multi-walled CNTs composites is mainly controlled by nanotubes if the ratio of nanotubes to PANI exceeds a percolation limit. As in this study the amount of SWCNT in the multilayer electrode is beyond the percolation limit, hence, PANI is just accountable for the proton conductivity. It is believed that the interpenetration of the several layers results in a suitable proton conductivity and no wrapping of the nanotubes by PANI occurs. On the other hand, the strong interpenetration leads to an analytical problem such that the layers are not observable individually using electron microscopy techniques.

The performance (Fig. 6) of the prepared Pt/SWCNT–Pt/PANI membrane was tested in an in-house built PEM fuel cell test bench. The multilayer electrode was used as a cathode and a standard Pt/CB catalyst and Nafion® ionomer was used at the anode side. The Pt loadings were 0.06 mg cm$^{-2}$ at the cathode and 0.7 mg cm$^{-2}$ at the anode, respectively. The performance data were collected at a H$_2$



**Fig. 5.** SEM micrograph of a Pt/SWCNT and Pt/PANI electrode on a Nafion® membrane.
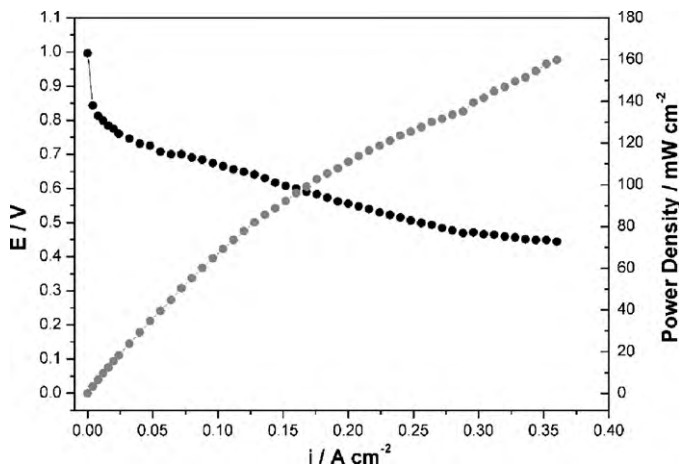


**Fig. 6.** Polarization (black) and power density (grey) curve of fuel cell with multilayer cathode. Fuel cell temperature: 75 °C, humidifier temperature: 80 °C.

flow rate of 183 ml min$^{-1}$ and a O$_2$ flow rate of 86 ml min$^{-1}$. The MEA yielded a peak power density of 160 mW cm$^{-2}$ at the cathode. The power density divided by the cathode's Pt loading gives a Pt utilization of 2663 mW mg$^{-1}$. To our knowledge, we believe that this value is the highest obtained for electrodes designed by a sprayed layer-by-layer assembly. An important note – the parameters of the fuel cell setup and the spraying technique are not fully optimized, we believe that higher Pt utilization could be expected at optimal preparation and testing conditions.

Taylor et al. [13] tested dipped LBL films of Pt/SWNCT + Nafion® and PANI at the anode side. The peak power density of the 400 bilayers was 127 mW cm$^{-2}$ at a Pt utilization of 2540 mW mg$^{-1}$. It should be mentioned that the two results are not completely comparable, because of the difference in the preparation and the use of the specifically prepared electrodes on different sides and the presence of Nafion® in the last study. Nevertheless, both studies show that LBL or spray coating electrodes can significantly increase the Pt utilization either on the anode or cathode side. Normally, the cathode is considered to be a more critical part if the catalytic activity of the catalyst material is low. This has not been the case with the multilayer MEA, so a high catalytic activity is estimated.

The high Pt utilization verifies the capacity of the spray coating method. The absence of Nafion® ionomer at the cathode also demonstrates that the proton conductivity in the layer can be handled by other conductive polymers like PANI. The advantages of using polymers are the facile tunability of their conductivity and their relatively low costs. The 1D supports open the possibility to invent new structures that can further improve the utilization on a high level.

## 4. Conclusions

The polyol method was used to deposit Pt nanoparticles on PANI-f and SWCNTs. The average particle size was estimated to be 4.0 and 4.8 nm, respectively. Thanks to the spray coating method, alternating layers of Pt/PANI and Pt/SWCNT on a Nafion® membrane could be assembled. The presence of an additional ionomer in the electrode layer besides PANI was not necessary for an adequate proton conductivity. The 1D supports created a 3D network which enhanced the Pt utilization compared to conventionally prepared PEMFC electrodes by a factor of 3. The good performance data showed the applicability of the spray coating technique as high potential MEA preparation technique, which could probably used for in-line production of MEAs. This method is fast and not equally time-consuming like the conventional dipping LBL technique. In contrast to the sprayed LBL method, excessive and not just adsorbed material sticks on the membrane and the loss of initial material could be reduced. As no electron transport is expected by PANI in the presence of a higher amount of carbon nanotubes, the decoration of PANI with noble metal particles does not seem to be necessary. This would lead to a further decrease of the Pt amount used in a MEA.

## References

[1] J. Larminie, A. Dicks, Fuel Cell Systems Explained, first ed., John Wiley & Sons Ltd, UK, 2001.
[2] J.-H. Wee, Renew. Sust. Energy Rev. 11 (2007) 1720–1738.
[3] S. Srinivasan, E.A. Ticianelli, C.R. Derouin, A. Redondo, J. Power Sources 22 (1988) 359–375.
[4] S. Srinivasan, O.A. Velev, A. Parthasarathy, D.J. Manko, A.J. Appleby, J. Power Sources 36 (1991) 299–320.
[5] R. O'Hayre, D.R. Barnett, F.F. Prinz, J. Electrochem. Soc. 152 (2) (2005) A439–A444.
[6] A.D. Taylor, E.Y. Kim, V.P. Humes, J. Kizuka, L.T. Thompson, J. Power Sources 171 (2007) 101–106.
[7] S. Towne, V. Viswanahan, J. Holbery, P. Rieke, J. Power Sources 171 (2007) 575–584.
[8] M. Cavarroc, A. Ennadjaoui, M. Mougenot, P. Brault, R. Escalier, Y. Tessier, J. Durand, S. Roualdès, T. Sauvage, C. Coutanceau, Electrochem. Commun. 11 (2009) 859–861.
[9] J.-H. Wee, K.-Y. Lee, S.H. Kim, J. Power Sources 165 (2007) 667–677.
[10] R. O'Hayre, S.-J. Lee, S.-W. Cha, F.B. Prinz, J. Power Sources 109 (2002) 483–493.
[11] M. Michel, A. Taylor, R. Sekol, P. Podsiadlo, P. Ho, N. Kotov, L. Thompson, Adv. Mater. 19 (2007) 3859–3864.
[12] M. Michel, F. Ettingshausen, F. Scheiba, A. Wolz, C. Roth, Phys. Chem. Chem. Phys. 10 (2008) 3796–3801.
[13] A.D. Taylor, M. Michel, R.C. Sekol, J.M. Kizuka, N.A. Kotov, L.T. Thompson, Adv. Funct. Mater. 18 (2008) 3003–3009.
[14] G. Decher, Science 277 (1997) 1232–1237.
[15] J.B. Schlenoff, S.T. Dubas, T. Farhat, Langmuir 16 (26) (2000) 9968–9969.
[16] A. Izquierdo, S.S. Ono, J.-C. Voegel, P. Schaaf, G. Decher, Langmuir 21 (16) (2005) 7558–7567.
[17] E. Antolini, E.R. Gonzalez, Appl. Catal. A 365 (2009) 1–19.
[18] A. Rahy, D.J. Yang, Mater. Lett. 62 (2008) 4311–4314.
[19] Z.W. Chen, L.B. Xu, W.Z. Li, M. Waje, Y.S. Yan, Nanotechnology 17 (20) (2006) 5254–5259.
[20] B. Rajesh, K.R. Thampi, J.M. Bonard, H.J. Mathieu, N. Xanthopoulos, B. Viswanathan, Electrochem. Solid-State Lett. 7 (11) (2004) A404–A407.
[21] L.M. Roen, C.H. Paik, T.D. Jarvi, Electrochem. Solid-State Lett. 7 (1) (2004) A19–A22.
[22] X. Wang, W. Li, Z. Chen, M. Waje, Y. Yan, J. Power Sources 158 (2006) 154–159.
[23] L. Brožová, P. Holler, J. Kovářová, J. Stejskal, M. Trochová, Polym. Degrad. Stab. 93 (2008) 592–600.
[24] J. Stejskal, R.G. Gilbert, Pure Appl. Chem. 74 (5) (2002) 857–867.
[25] L.J. van der Pauw, Philips Res. Rep. 13 (1) (1958) 1–9.
[26] D. Li, R.B. Kaner, Chem. Commun. (2005) 3286–3288.
[27] F. Scheiba, N. Benker, U. Kunz, C. Roth, H. Fuess, J. Power Sources 177 (2008) 273–280.
[28] D. Li, R.B. Kaner, J. Am. Chem. Soc. 128 (3) (2006) 968–975.
[29] J. Stejskal, I. Sapurina, Pure Appl. Chem. 77 (5) (2005) 815–826.
[30] M. Peuckert, T. Yoneda, R.A. Dalla Betta, M. Boudart, J. Electrochem. Soc. 133 (5) (1986) 944–947.
[31] I. Sapurina, J. Stejskal, Chem. Pap. 63 (5) (2009) 579–585.